Journal of Robotics and Control (JRC)
Volume 3, Issue 3, May 2022
ISSN: 2715-5072, DOI: 10.18196/jrc.v3i3.14585

Enhancement of the Tracking Performance for Robot Manipulator by Using the Feed-forward Scheme and Reasonable Switching Mechanism

Ha Quang Thinh Ngo [1,2,*], Minh Hoang Nguyen [1,2]
[1] Department of Mechatronics, Faculty of Mechanical Engineering, Ho Chi Minh City University of Technology (HCMUT), 268 Ly Thuong Kiet Street, District 10, Ho Chi Minh City, Vietnam
[2] Vietnam National University Ho Chi Minh City (VNU-HCM), Linh Trung Ward, Thu Duc District, Ho Chi Minh City, Vietnam
*Corresponding author

***Abstract*—Robot manipulator has become an exciting topic for many researchers during several decades. They have investigated the advanced algorithms such as sliding mode control, neural network, or genetic scheme to implement these developments. However, they lacked the integration of these algorithms to explore many potential expansions. Simultaneously, the complicated system requires a lot of computational costs, which is not always supported. Therefore, this paper presents a novel design of switching mechanisms to control the robot manipulator. This investigation is expected to achieve superior performance by flexibly adjusting various strategies for better selection. The Proportional-Integral-Derivative (PID) scheme is well-known, easy to implement, and ensures rapid computation while it might not have much control effect. The advanced interval type-2 fuzzy sliding mode control properly deals with nonlinear factors and disturbances. Consequently, the PID scheme is switched when the tracking error is less than the threshold or is far from the target. Otherwise, the interval type-2 fuzzy sliding mode control scheme is activated to cope with unknown factors. The main contributions of this paper are (i) the recommendation of a suitable switching mechanism to drive the robot manipulator, (ii) the successful integration of the interval type-2 fuzzy sliding mode control to track the desired trajectory, and (iii) the launching of several tests to validate the proposed controller with robot model. From these achievements, it would be stated that the proposed approach is effective in tracking performance, robust in disturbance-rejection, and feasible in practical implementation.**

Keywords*—Industrial manipulator; Advanced algorithm; servo system; Intelligent switching; Positioning control.

I. INTRODUCTION

Since the concept of fuzzy logic control was first presented [1, 2], there are many related pieces of research in this domain. Most of them have considerably contributed to the successful development for knowledge of mankind. Authors in [3] have investigated the earlier fuzzy logic controller, which emerged in many industrial applications for system modeling and the real world. Later, this control scheme which was adopted as a type-1 fuzzy logic system (FLS), was embedded into a water treatment plant in Japan [4-7]. After several years, many developers noticed that one of the main disadvantages in the design of type-1 FLS is the non-flexible shape of membership functions. Besides, it is unreasonable that increasing the number of rules and membership functions is larger than a certain threshold. This causes to increase in the complexity of the fuzzy system whilst there is no more effect on the outputs.

Therefore, it was motivated to suggest the improved FLS to deal with uncertainties in fuzzy control. Then, type-2 FLS was invented by adding an extra degree of freedom to incorporate the uncertain factors [8]. The membership is graded to increase the capability to proceed with inexact data in a logically correct manner [9, 10]. However, the type-2 FLS still has some drawbacks due to the mathematical complexity. A simpler design of this scheme was represented as interval type-2 FLS in which the uncertain factors were mapped into 3D-space while the value of each point in the membership function was matched in 2D-space. They inherit the mathematical expression from type-1 FLS, although it is simpler than type-2 FLS. It should be noted that the block of defuzzification in type-1 FLS is substituted by the output of the processing block in type-2 FLS. This block plays an important role in matching the fuzzy set of type-2 FLS and one of the type-1 FLS. In detail, it maps the uncertainties to an interval between the upper membership function and the lower one. Recently, some researchers have studied related topics to compare them. The competitive robustness between type-1 FLS and interval type-2 FLS has been mentioned in [11-13]. It was declared that a smaller approximation error could be achieved by interval type-2 FLS through the selective motivation depending on applications. In [14], a systematic view between singleton type-1 FLS, non-singleton type-1 FLS, and singleton type-2 FLS under the presence of noise was performed. Some criticisms to compare were created in a common framework even though a regular methodology to learn three styles were addressed.

The motivations of our approach are to deploy a reasonable mechanism to select and integrate the feed-forward strategy into the industrial manipulator. Superior performance is expected to achieve owing to the advantages of these schemes. The traditional PID scheme is activated when the tracking error is less than the threshold, or it is far from the destination. Or else, the scheme of interval type-2 fuzzy sliding mode control is triggered to deal with unknown factors. Feed-forward control is an advanced control scheme that is well-suited for processes.

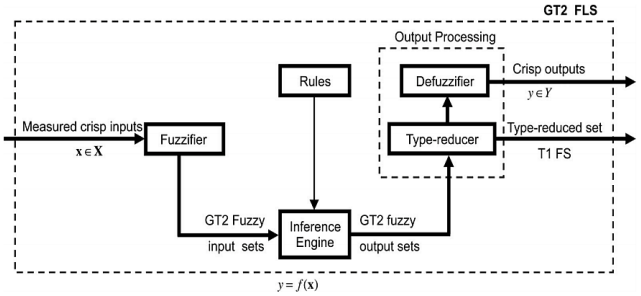

Fig. 1. Inside structure of type-2 FLS.

II. BACKGROUND WORKS

In general, a conventional type-2 FLS focuses on the uncertain membership functions; however, it evaluates these uncertainties nonuniformly. The membership function of type-2 FLS is depicted in 3D space where the values on the z-axis resemble. Commonly, it could be illustrated in four different ways such as points, wavy slices, horizontal slices, and vertical slices. To explain clearly, Fig. 1 shows the structure of type-2 FLS that includes several blocks. The fuzzifier process matches a crisp input vector which consists of multi-inputs, into type-2 fuzzy sets. The inference engine merges rules and connects from input type-2 FLS to output type-2 FLS. The outputs of the fuzzy inference engine are a type-2 fuzzy set.

In the interval type-2 FLS, it is assumed that there is uncertainty in determining the values of the membership. Thus, the concept of modeling uncertainty has been investigated in recent times. The most famous algorithms for estimating the output of an interval type-2 FLS are Karnik-Mendel (KM) [19], Nie-Tan (NT) [20], and Wu-Mendel (WM) [21]. The KM approach mostly uses the type reduction method for type-2 FLS in order to compute the output. Later, many investigations have been introduced, such α-cut algorithm [22-25], to solve the problem of weighted value. In the other method [26, 27], the KM approach was to generate a boundary function which was proved to be greater and more practicable. The NT method calculates the union of a fired rule for output. Owing to this, the mean of the lower membership function and the upper membership function is computed. Conversely, the WM method was innovated to push the process of type-2 FLS by eliminating the computational burden of type reduction. The number of iterations before convergence should be cut down. Additionally, the uncertainty bounds are evaluated by mathematical formulas for both inner and outer sets [28-32].

III. FUNDAMENTALS OF INTERVAL TYPE-2 FUZZY LOGIC SYSTEM

Theoretically speaking, the idea of an interval type-2 fuzzy logic system is well-depicted in [33, 34]. Thus, a short explanation of the interval type-2 FLS is mentioned in this section. We consider that in the universal set X, a type-2 FLS is symbolized as $\tilde{A}$, which is characterized by a membership function (MF) $u_{\tilde{A}}(x)$ of type-2 FLS. This function $u_{\tilde{A}}(x)$ could be stated as a secondary MF. Commonly, the MF in type-1 varies in a range of [0, 1].

TABLE I. THE STATE-OF-ART OVERVIEW OF RELATED RESEARCH

Application	Author(s)	Achievement(s)	Drawback(s)
Robot Manipulator	Mien Van et al. [15]	A novel control methodology for tracking control of manipulator was designed to maintain the high performance in terms of high robustness, fast transient response, and finite-time convergence	It requires the effective measurement of noises and a better sensor as well as a tuning mechanism to get the optimal values for the major coefficients in this method
Electric Vehicle	A. Aziz K. et al. [16]	An adaptive interval type-2 FLS based on the online learning approach was declared to ensure stability and overcome the shortcomings of the gradient descent. This method could deal with uncertain nonlinear systems.	The optimal learning rate and the critical stability should be discussed
Mobile Robot	Juang C. F. et al. [17]	For the wheeled mobile robot wall-following control, a novel reinforcement and optimized fuzzy controller design method, which consists of interval type-2 fuzzy sets to increase the robustness, and an online interval type-2 fuzzy clustering to generate rules automatically was proposed.	The problems such as navigation or obstacle avoidance for the autonomous system did not take into account.
Hexapod	Wu Chung S. et al [18]	A method of data-driven multi-objective evolutionary interval type-2 FLS was considered for both system performance and rule interpretability. The achievements are that the structure of interval type-2 FLS was incrementally generated to reduce the parameter search space, and a new constrained objective function to enhance the distinguishability of fuzzy sets was suggested.	In a large number of control trials, the challenges of real regression and classification in an unstructured environment must be improved.

$$\tilde{A} = \int x \in X \frac{u_{\tilde{A}}(x)}{x} = \int x \in X \frac{\left[\int u \in J_x^{f_x(x)/u}\right]}{x} \quad J_x \subseteq [0,1] \tag{1}$$

where $f_x(u)$ is a second grade or the amplitude of a secondary MF and $0 \leq f_x(u) \leq 1$. Jx is the primary membership of x, with $u \in J_x \subseteq [0, 1]$ for $\forall x \in X$; u is a fuzzy set in [0, 1].

As a result, the domain of a secondary MF is called the primary membership of x. If $f_x(u) = 1$, $\forall u \in J_x \subseteq [0, 1]$, then the secondary MFs are interval sets so that $u_{\tilde{A}}(x)$ in (1) could be assumed as an interval type-2 MF. Thus, a type-2 FLS is rewritten as follows.

$$\tilde{A} = \int x \in X \frac{u_{\tilde{A}}(x)}{x} = \int x \in X \frac{\left[\int u \in J_x^{1/u}\right]}{x} \quad J_x \subseteq [0,1] \tag{2}$$

Moreover, the Gaussian-based shape for primary MF with uncertain values of mean and standard deviation, which have an interval type-2 secondary MF, could be named an interval type-2 Gaussian MF [35-38]. The mathematical expression of an interval type-2 Gaussian MF with the uncertainties in mean m and standard deviation σ is performed as

$$u_{\tilde{A}}(x) = exp\left[-\frac{1}{2}\left(\frac{x-m}{\sigma}\right)^2\right], \text{ m} \in [m_1, m_2]. \tag{3}$$

From Fig. 2, the grey region has been named a footprint of uncertainty (FOU), and it exists the boundary values such as an upper MF $\bar{u}_{\tilde{A}}(x)$ and a lower MF $\underline{u}_{\tilde{A}}(x)$ correspondingly. In this case, equation (1) is indicated as

$$\tilde{A} = \int x \in X \frac{\int \mu \in [u_{\tilde{A}}(x), \bar{u}_{\tilde{A}}(x)]^{1/u}}{x} \tag{4}$$

The structure of type-2 FLS is shown in Fig. 3. It has been known that there are several main components such as fuzzifier for inputs, rule base and inference engine for processing, type-reducer, and fuzzified for outputs [39, 40]. After passing all steps, a crisp value could be obtained in the output port of the controller.

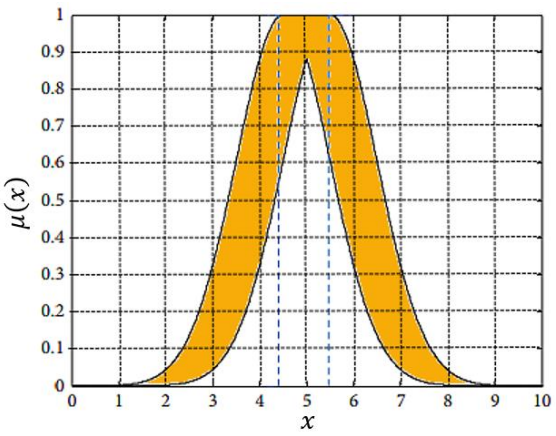

Fig. 2. Description of an interval type-2 Gaussian MF

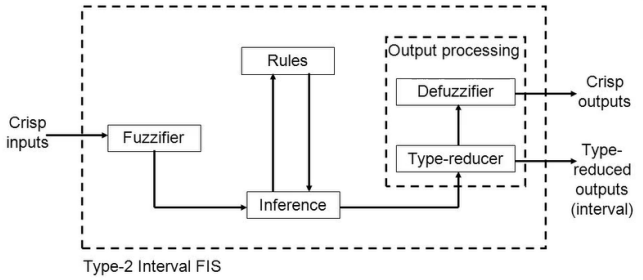

Fig. 3. A framework of a type-2 FLS.

IV. PROPOSED METHOD

Our purpose is to design an advanced control scheme in order to enhance system performance. The idea to integrate both the popular control strategy in the industry and the interval type-2 fuzzy sliding mode control (FSMC) is proposed in this research. Initially, the conventional scheme such Proportional-Integral-Derivative (PID) is chosen to drive the system if the target position is still far or the tracking error is less than the threshold. When this system is closely reaching to target or a larger error occurs, the interval type-2 FSMC is activated to achieve high performance. It is expected to lessen the steady-state error, overshoot in the transient period, and ameliorate the system response to

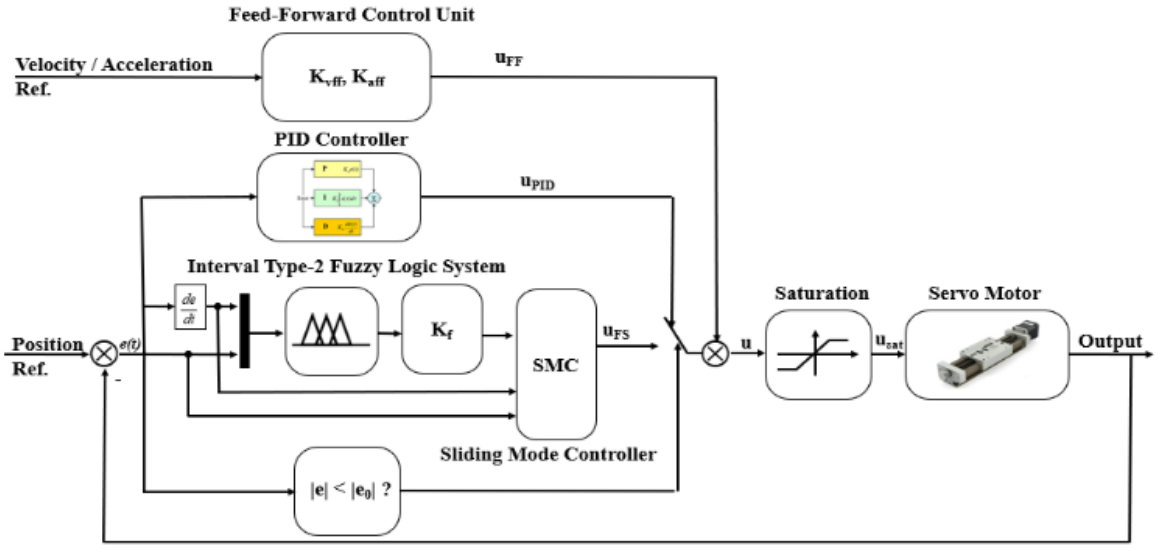

Fig. 4. The overall structure of the proposed system.

counteract disturbed parametric and external disturbances. The switching mechanism to alternative trigger the proper control scheme is suggested. Actively, it is continuously switched between two control strategies to provide flexible control commands. Also, the feed-forward scheme is implemented because its characteristics are well-suited for the motion control system. This additional scheme would proactively adjust by releasing an appropriate response at the proper time. In Fig. 4, the whole structure of our controller, which is mentioned above, is shown. As a result, it is able to minimize the negative effects on the servo system.

A. The concept of a switching mechanism

According to the desired performance, a novel innovation of integrating the schemes, both common control and advanced technique, is recommended. It is hopefully expected that the ease-to-use of the PID scheme and the superior. The performance of type-2 FLS could drive the servo system stably and perfectly. The switching engine is manipulated by the tracking error threshold e_0 that is identified by expert-based knowledge. The output control signal u of our controller is depicted as

$$u = switching(u_{FS}, u_{PID}) + u_{FF} \quad (5)$$

$$u_{sat} = sat(u) \quad (6)$$

where u_{FS} is the output control signal from interval type-2 FSMC, u_{PID} is the output control signal from the PID scheme, u_{FF} is the output control signal from a feed-forward scheme, u_{sat} is the output control signal from the saturation unit.

Algorithm 1. Pseudocode of the Proposed Method.

Input:
K_{vff}, K_{aff} ← coefficients from a feed-forward scheme
K_P, K_I, K_D ← coefficients from PID scheme
$_{If}$ ← coefficients from interval type-2 FLS
e_0 ← threshold value of tracking error
Output:
u ← output control
Initialize:
Position $_{reference}$ ← *motion profile generator*
Procedure
Begin
1 While *InMotion* Do
2 If *((|e| < |e₀|) or farfromtarget)* then
3 $u \leftarrow u_{PID} + u_{FF}$ // switch to PID scheme
4 Else
5 $u \leftarrow u_{FS} + u_{FF}$ // switch to interval type-2 FSMC scheme
6 $u_{sat} \leftarrow sat(u)$ // compute the saturated control signal
End

where, K_{vff}, K_{aff}: the tuning gains of velocity and acceleration in a feed-forward scheme. K_P, K_I, K_D: the tuning gains of a proportional, integral, and derivative components in the PID scheme. K_f is the tuning gain of the interval type-2 FLS scheme

In our experience, the feed-forward control is well-suited for a motion system that is routinely driven by a servo mechanism. With this implementation, the feed-forward architecture enables proactive adjustments. Those modifications deliver an appropriate response at the proper time, and they are thereby able to minimize the negative effects on the servo system. To eliminate the unexpected signal, the saturation unit is additionally implemented to ensure that the output command from the proposed controller is in range.

The entire algorithm is represented as above. At the initial stage, the tuning parameters, which require a lot of experience to select, are inserted. Then, when the motion profile is firstly generated, the whole system is activated. The proposed controller continuously compares the value of the tracking error and its threshold in order to decide which scheme is chosen. The threshold of error plays as a boundary value to maintain the high performance of this system. Its value depends on the system state of practical tests and expert-based knowledge. If the tracking error is less than this threshold or it is far from the target, the PID scheme is optionally deployed. Regularly, the velocity profile of the motion system is classified into three sections acceleration, constant speed, and deceleration. The definition of "far from target" is determined when the period of the velocity profile is either acceleration or constant speed. Otherwise, it reaches the near target. If those conditions are not satisfied, the type-2 FLS scheme is triggered to manipulate the servo system. Finally, the control signal is saturated to guarantee the physical limitations of both the servo motor and mechanical framework.

B. The implementation of the traditional PID control scheme

It is well-known that the PID strategy is one of the most popular methods to drive the automated system. The benefit of this control scheme is to reduce the burden of computation owing to the complicated expression of math. Moreover, the cycle time for processing is also shortened to ensure the real-time characteristic. It could be widely applied in robotics, servo mechanism, or high precision machining system. The output control of this scheme is

$$u_{PID} = K_P e + K_I \int e dt + K_D \frac{de}{dt} \quad (7)$$

C. The design of interval type-2 FSMC

In our research, the target to control is a two-link robot arm, as shown in Fig. 5. It is considered that this two-link rigid robot consists of the first link mounted on a fixed base and the second one connected to the end of the previous link.

The dynamic equation of this robot manipulator is

$$\begin{pmatrix}\ddot{q}_1\\ \ddot{q}_2\end{pmatrix} = \begin{pmatrix}M_{11} & M_{12}\\ M_{21} & M_{22}\end{pmatrix}^{-1}\left[\begin{pmatrix}u_1\\ u_2\end{pmatrix} - \begin{pmatrix}-k\dot{q}_2 & -k(\dot{q}_1+\dot{q}_2)\\ k\dot{q}_1 & 0\end{pmatrix}\begin{pmatrix}\dot{q}_1\\ \dot{q}_2\end{pmatrix}\right] \quad (8)$$

where,

$$M_{11} = m_1^T + 2m_3^T cos(q_2) + 2m_4^T sin(q_2) \quad (9)$$

$$M_{22} = m_2^T$$
$$M_{12} = M_{21} = m_2^T + m_3^T cos(q_2) + m_4^T sin(q_2)$$
$$k = m_3^T sin(q_2) - m_4^T cos(q_2)$$

and,

$$\begin{aligned} m_1^T &= I_1 + m_1 l_{c1}^2 + I_e + m_e l_{ce}^2 + m_e l_1^2 \\ m_2^T &= I_e + m_e l_{ce}^2 \\ m_3^T &= m_e l_1 l_{ce} cos(\delta_e) \\ m_4^T &= m_e l_1 l_{ce} sin(\delta_e) \end{aligned} \quad (10)$$

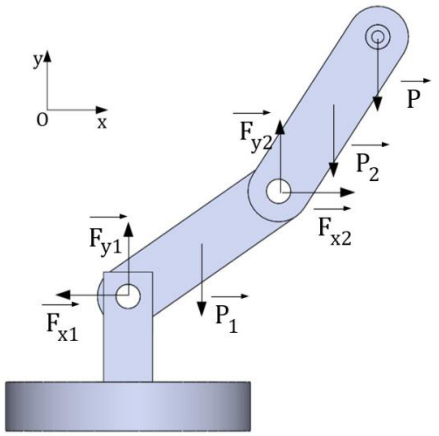

Fig. 5. Illustration of a two-link manipulator in a planar plane.

We assume that the vector of output $y \in R^2$, the vector of control input $u \in R^2$, and the vector of fully measurable state variable $x \in R^4$ are $y = [y_1 \quad y_2]^T = [q_1 \quad q_2]^T \in R^2$, $u = [u_1 \quad u_2]^T \in R^2$, $x = [q_1 \quad \dot{q}_1 \quad q_2 \quad \dot{q}_2]^T \in R^4$ and correspondingly.

Let us denote that $f_i(x), i = 1,2$; $g_{ij}(x), i,j = 1,2$ and are the continuous nonlinear functions belongC^1.

$$\begin{aligned} F(x) &= \begin{bmatrix} f_1(x) \\ f_2(x) \end{bmatrix} \\ &= -M \begin{bmatrix} -k\dot{q}_2 & -k(\dot{q}_1 + \dot{q}_2) \\ k\dot{q}_1 & 0 \end{bmatrix} \begin{bmatrix} \dot{q}_1 \\ \dot{q}_2 \end{bmatrix} \end{aligned} \quad (11)$$
$$G(x) = \begin{bmatrix} g_{11}(x) & g_{12}(x) \\ g_{21}(x) & g_{22}(x) \end{bmatrix} = M^{-1} = \begin{bmatrix} M_{11} & M_{12} \\ M_{21} & M_{22} \end{bmatrix}$$

Assumption 1: If the matrix $G(x)$ is positive definite, then there is always a value $\sigma_0 > 0, \sigma_0 \in R$ so that $G(x) \geq \sigma_0 I_p$ with I_p being a unit matrix.

Assumption 2: The reference trajectory $y_{di}, i = 1,2$ is a known function with respect to time and continuously.

Therefore, since the matrix M is positive definite, then it is often regular and $G(x) = M^{-1}$is positive definite too.

Owing to the existence of nonlinear functions $f_i(x)$, $g_{ij}(x)$, it is hard to achieve high performance for this system. Our solution is to approximate these unknown functions by using the type-2 FLS as follows.

$$\hat{f}_i(x, \tilde{\alpha}_{fi}) = \xi_{fi}^T(x)\tilde{\alpha}_{fi}, \quad \text{i} = 1, \ldots, \text{p}, \quad (12)$$

$$\tilde{g}_{ij}(x, \tilde{\alpha}_{gij}) = \xi_{gij}^T(x)\tilde{\alpha}_{gij}, \quad \text{i, j} = 1, \ldots, \text{p},$$

where, $\xi_{fi}^T(x)$ and $\xi_{gij}^T(x)$ are fuzzy basis vectors fixed by an expert $\tilde{\alpha}_{fi}$ and $\tilde{\alpha}_{gij}$ are the respective adjustable parameter vectors of each interval type-2 fuzzy system. The supremum of those parameters is defined as

$$\begin{aligned} \tilde{\alpha}_{fi}^* &= arg \min_{\tilde{\alpha}_{fi}} \left\{ \sup_{x \in D_X} \left| f_i(x) - \hat{f}_i(x, \tilde{\alpha}_{fi}) \right| \right\} \\ \tilde{\alpha}_{gij}^* &= arg \min_{\tilde{\alpha}_{gij}} \left\{ \sup_{x \in D_X} \left| g_{ij}(x) - \hat{g}_{ij}(x, \tilde{\alpha}_{gij}) \right| \right\} \end{aligned} \quad (13)$$

where, $\tilde{\alpha}_{fi}^*$ and $\tilde{\alpha}_{gij}^*$are the optimal parameters of $\tilde{\alpha}_{fi}$ and $\tilde{\alpha}_{gij}$ respectively. We define the parameters of estimation errors as

$$\begin{aligned} \tilde{\tilde{\alpha}}_{ij} &= \tilde{\alpha}_{fi}^* - \tilde{\alpha}_{fi}, \\ \tilde{\tilde{\alpha}}_{gij} &= \tilde{\alpha}_{gij}^* - \tilde{\alpha}_{gij} \end{aligned} \quad (14)$$

and

$$\begin{aligned} \varepsilon_{fi}(x) &= f_i(x) - \hat{f}_i(x, \tilde{\alpha}_{fi}^*), \\ \varepsilon_{gfi}(x) &= g_{ij}(x) - \hat{g}_{ij}(x, \tilde{\alpha}_{gij}^*), \end{aligned} \quad (15)$$

where, $\varepsilon_{fi}(x), \varepsilon_{gfi}(x)$ are the minimum fuzzy pproximation errors

Assumption 3: It is assumed that the minimum approximation errors are bounded for all $x \in D_X$ with a compact set D_X; that is,

$$\begin{aligned} \left|\varepsilon_{fi}(x)\right| &\leq \bar{\varepsilon}_{fi} \\ \left|\varepsilon_{gij}(x)\right| &\leq \bar{\varepsilon}_{gij} \end{aligned} \forall x \in D_X \quad (16)$$

where $\bar{\varepsilon}_{fi}$, ε_{gij} and are constants.

Hence, these parameters and functions are expressed as

$$\begin{aligned} \hat{F}(x, \tilde{\alpha}_f) &= \left[\hat{f}_1(x, \tilde{\alpha}_{f1}) \quad \hat{f}_p(x, \tilde{\alpha}_{fp})\right]^T \\ \hat{G}(x, \tilde{\alpha}_g) &= \begin{bmatrix} \hat{g}_{11}(x, \tilde{\alpha}_{g11}) & \hat{g}_{12}(x, \tilde{\alpha}_{g12}) \\ \hat{g}_{21}(x, \tilde{\alpha}_{g21}) & \hat{g}_{22}(x, \tilde{\alpha}_{g22}) \end{bmatrix} \\ \varepsilon_f(x) &= [\varepsilon_{f1}(x) \quad \varepsilon_{f2}(x)]^T \\ \varepsilon_g(x) &= \begin{bmatrix} \varepsilon_{g11}(x) & \varepsilon_{g12}(x) \\ \varepsilon_{g21}(x) & \varepsilon_{g22}(x) \end{bmatrix} \\ \bar{\varepsilon}_f(x) &= [\bar{\varepsilon}_{f1} \quad \bar{\varepsilon}_{f2}]^T \\ \bar{\varepsilon}_g(x) &= \begin{bmatrix} \bar{\varepsilon}_{g11} & \bar{\varepsilon}_{g12} \\ \bar{\varepsilon}_{g21} & \bar{\varepsilon}_{g22} \end{bmatrix} \end{aligned} \quad (17)$$

Thus, the nonlinear functions are described as

$$\begin{aligned} F(x) - \hat{F}(x, \tilde{\alpha}_f) &= \hat{F}(x, \tilde{\alpha}_f^*) - \hat{F}(x, \tilde{\alpha}_f) + \varepsilon_f(x) \\ G(x) - \hat{G}(x, \tilde{\alpha}_g) &= \hat{G}(x, \tilde{\alpha}_g^*) - \hat{G}(x, \tilde{\alpha}_g) + \varepsilon_g(x) \end{aligned} \quad (18)$$

The tracking error $e^T = [e_1 \quad e_2]^T$ is identified from the desired input and the actual output as follows.

$$\begin{aligned} e_1(t) &= y_{d1}(t) - y_1(t) \\ e_2(t) &= y_{d2}(t) - y_2(t) \end{aligned} \quad (19)$$

Similarly, the sliding surface $s^T = [s_1 \quad s_2]^T$ is determined as

$$\begin{aligned} s_1(t) &= \left(\frac{d}{dt} + \lambda_1\right) e_1(t) \\ s_2(t) &= \left(\frac{d}{dt} + \lambda_2\right) e_2(t) \end{aligned} \qquad \lambda_1, \lambda_2 > 0 \tag{20}$$

Taking the first derivative of these sliding surfaces, we have

$$\begin{aligned} \dot{s}_1 &= v_1 - f_1(x) - \sum_{j=1}^{P} g_{1j}(x) u_j \\ \dot{s}_P &= v_P - f_P(x) - \sum_{j=1}^{P} g_{pj}(x) u_j \end{aligned} \tag{21}$$

where $v_1, \dots, v_p$ are given as following

$$\begin{aligned} v_1 &= \dot{y}_{d1} + \dot{\lambda}_1 \dot{e}_{1_1} \\ v_2 &= \dot{y}_{d2} + \dot{\lambda}_2 \dot{e}_2 \end{aligned} \tag{22}$$

Our concept is to design a sliding mode controller to drive this system stably and timely. This control strategy consists of two components, such equivalent scheme, and a reaching scheme. The equivalent control u_{eq} is to deploy when the system state locates on the sliding surface. The sliding control $u_{sliding}$ is to force the system state for reaching to the surface. Therefore, the control signal u_{FS} is

$$u_{FS} = u_{eq} + u_{sliding} \tag{23}$$

If the system state stays on the sliding surface ($\dot{s} = 0$), the control signal u would be u_{eq} which is estimated as

$$\begin{aligned} u_{eq} &= \hat{G}(x, \tilde{\alpha}_g)\big[\varepsilon_0 I_p \\ &+ \hat{G}(x, \tilde{\alpha}_g)\hat{G}^T(x, \tilde{\alpha}_g)\big]^{-1}.\big[-\hat{F}(x, \tilde{\alpha}_f) + v \\ &+ K_0 sgn(s)\big] \end{aligned} \tag{24}$$

where, $K_0 = \begin{bmatrix} k_1 & 0 \\ 0 & k_2 \end{bmatrix}$ with k_1, $k_2 > 0$, ε_0 is a positive constant.

In this controller, equation (24) describes the estimation of nonlinear functions $\hat{F}(x, \tilde{\alpha}_f)$ $\hat{G}(x, \tilde{\alpha}_g)$ in place of the real term of nonlinear function $F(x)$ and $G(x)$.

When the system state leaves the surface, the sliding control signal $u_{sliding}$ is expected to drive its back.

$$u_{sliding} = \frac{s|s^T|(\bar{s}_f + \bar{s}_g|u_{eq}| + |u_0|)}{\sigma_0\|s\|^2 + \delta} \tag{25}$$

where u_0 is

$$\begin{aligned} u_0 &= \varepsilon_0\big[\varepsilon_0 I_p + \hat{G}(x, \tilde{\alpha}_g)\hat{G}^T(x, \tilde{\alpha}_g)\big]^{-1}.\big[-\hat{F}(x, \tilde{\alpha}_f) \\ &+ v + K_0 sgn(s)\big], \end{aligned} \tag{26}$$

and δ is a time-varying variable

Later, the adaptive rules to update the tuning parameters are identified as

$$\dot{\tilde{\alpha}}_{fi} = -\eta_{fi}\xi_{fi}(x)s_i, \tag{27}$$

$$\dot{\tilde{\alpha}}_{gij} = -\eta_{gij}\xi_{gij}(x)s_i u_{si}, \tag{28}$$

$$\dot{\delta} = -\eta_0 \frac{|s^T|(\bar{s}_f + \bar{s}_g|u_s| + |u_0|)}{\sigma_0\|s\|^2 + \delta}, \tag{29}$$

where, η_{fi}, η_{gij}, η_0 are positive values. The initial condition of δ is also positive.

Several mathematical expressions could be carried out,

$$\begin{aligned} \dot{s} = v - F(x) &- \big[G(x) - \hat{G}(x, \tilde{\alpha}_g)\big]u_{eq} \\ &- \hat{G}(x, \tilde{\alpha}_g)u_{eq} - \hat{G}(x)u_{sliding} \end{aligned} \tag{30}$$

Substituting the control term from the above equations, we have

$$\begin{aligned} \dot{s} = -K_0\, sgn(s) &- \big[F(x) - \hat{F}(x, \tilde{\alpha}_f)\big] \\ &- \big[G(x) - \hat{G}(x, \tilde{\alpha}_g)\big]u_{eq} + u_0 \\ &- \hat{G}(x)u_{sliding} \end{aligned} \tag{31}$$

Due to the mathematical transformation, the additional expression could be obtained as

$$\begin{aligned} &\hat{G}(x, \tilde{\alpha}_g)\hat{G}^T(x, \tilde{\alpha}_g)\big[\varepsilon_0 I_p + \hat{G}(x, \tilde{\alpha}_g)\hat{G}^T(x, \tilde{\alpha}_g)\big]^{-1} \\ &\quad = I_p - \varepsilon_0\big[\varepsilon_0 I_p + \hat{G}(x, \tilde{\alpha}_g)\hat{G}^T(x, \tilde{\alpha}_g)\big]^{-1} \end{aligned} \tag{32}$$

Therefore,

$$\begin{aligned} \dot{s} = -K_0\, sgn(s) &- \big[F(x, \tilde{\alpha}_f^*) - \hat{F}(x, \tilde{\alpha}_f)\big] \\ &- \big[G(x, \tilde{\alpha}_g^*) - \hat{G}(x, \tilde{\alpha}_g)\big]u_{eq} \\ &+ u_0 - \hat{G}(x)u_{sliding} + u_0 \\ &- \varepsilon_f(x) - \varepsilon_g(x)u_{eq} \end{aligned} \tag{33}$$

Then,

$$\begin{aligned} s^T\dot{s} = -s^T K_0\, sgn(s) &- \big(\xi_{f1}^T(x)\tilde{\bar{\alpha}}_{f1}s_1 + \xi_{f2}^T(x)\tilde{\bar{\alpha}}_{f2}s_2\big) \\ &- (\xi_{g11}^T(x)\tilde{\bar{\alpha}}_{g11}s_1 u_{eq1} \\ &+ \xi_{g12}^T(x)\tilde{\bar{\alpha}}_{g12}s_1 u_{eq2} \\ &+ \xi_{g21}^T(x)\tilde{\bar{\alpha}}_{g21}s_2 u_{eq1} \\ &+ \xi_{g22}^T(x)\tilde{\bar{\alpha}}_{g22}s_2 u_{eq2}) \\ &- s^T G(x)u_{sliding} + s^T u_0 \\ &- s^T\varepsilon_f(x) - s^T\varepsilon_g(x)u_{eq} \end{aligned} \tag{34}$$

The Lyapunov candidate function could be chosen as

$$\begin{aligned} V &= \frac{1}{2}s^T s + \frac{1}{2}\left(\frac{1}{\eta_{f1}}\tilde{\bar{\alpha}}_{f1}^T\tilde{\bar{\alpha}}_{f1} + \frac{1}{\eta_{f2}}\tilde{\bar{\alpha}}_{f2}^T\tilde{\bar{\alpha}}_{f2}\right) \\ &+ \frac{1}{2}\left(\frac{1}{\eta_{g11}}\tilde{\bar{\alpha}}_{g11}^T\tilde{\bar{\alpha}}_{g11}\right. \\ &+ \frac{1}{\eta_{g12}}\tilde{\bar{\alpha}}_{g12}^T\tilde{\bar{\alpha}}_{g12} + \frac{1}{\eta_{g21}}\tilde{\bar{\alpha}}_{g21}^T\tilde{\bar{\alpha}}_{g21} \\ &\left.+ \frac{1}{\eta_{g22}}\tilde{\bar{\alpha}}_{g22}^T\tilde{\bar{\alpha}}_{g22}\right) + \frac{1}{2\eta_0}\delta^2 \end{aligned} \tag{35}$$

Taking the first derivative, we have

$$\begin{aligned}\dot{V} &= s^T\dot{s} - \left(\frac{1}{\eta_{f1}}\tilde{\bar{\alpha}}_{f1}^T\dot{\tilde{\bar{\alpha}}}_{f1} + \frac{1}{\eta_{f2}}\tilde{\bar{\alpha}}_{f2}^T\dot{\tilde{\bar{\alpha}}}_{f2}\right) \\ &- \left(\frac{1}{\eta_{g11}}\tilde{\bar{\alpha}}_{g11}^T\dot{\tilde{\bar{\alpha}}}_{g11} + \frac{1}{\eta_{g12}}\tilde{\bar{\alpha}}_{g12}^T\dot{\tilde{\bar{\alpha}}}_{g12} + \frac{1}{\eta_{g21}}\tilde{\bar{\alpha}}_{g21}^T\dot{\tilde{\bar{\alpha}}}_{g21}\right. \\ &\left. + \frac{1}{\eta_{g22}}\tilde{\bar{\alpha}}_{g22}^T\dot{\tilde{\bar{\alpha}}}_{g22}\right) + \frac{1}{\eta_0}\delta\dot{\delta}\end{aligned} \quad (36)$$

Equation (36) could be re-written as

$$\dot{V} = s^T K_0\, sgn(s) + \dot{V}_1 + \dot{V}_2 \quad (37)$$

where,

$$\begin{aligned}\dot{V}_1 = &-\tilde{\bar{\alpha}}_{f1}^T\left(\xi_{f1}(x)s_1 + \frac{1}{\eta_{f2}}\dot{\tilde{\bar{\alpha}}}_{f2}\right) \\ &- \tilde{\bar{\alpha}}_{f2}^T\left(\xi_{f2}(x)s_2 + \frac{1}{\eta_{f2}}\dot{\tilde{\bar{\alpha}}}_{f2}\right) \\ &- \tilde{\bar{\alpha}}_{g11}^T\left(\xi_{g11}(x)s_1u_{eq1} + \frac{1}{\eta_{g11}}\dot{\tilde{\bar{\alpha}}}_{g11}\right) \\ &- \tilde{\bar{\alpha}}_{g12}^T\left(\xi_{g12}(x)s_1u_{eq2} + \frac{1}{\eta_{g12}}\dot{\tilde{\bar{\alpha}}}_{g12}\right) \\ &- \tilde{\bar{\alpha}}_{g21}^T\left(\xi_{g21}(x)s_2u_{eq1} + \frac{1}{\eta_{g21}}\dot{\tilde{\bar{\alpha}}}_{g21}\right) \\ &- \tilde{\bar{\alpha}}_{g22}^T\left(\xi_{g22}(x)s_2u_{eq2} + \frac{1}{\eta_{g22}}\dot{\tilde{\bar{\alpha}}}_{g22}\right)\end{aligned}$$

$$\begin{aligned}\dot{V}_2 = &-s^TG(x)u_{sliding} + s^Tu_0 - s^T\varepsilon_f(x) - s^T\varepsilon_g(x)u_{eq} \\ &+ \frac{1}{\eta_0}\delta\dot{\delta}\end{aligned}$$

From these adaptive rules, it is confirmed that

$$\dot{V}_1 = 0 \quad (38)$$

In the other hand, we have

$$\begin{aligned}s^TG(x)u_{sliding} \geq |s^T|.&\left(\bar{\varepsilon}_f + \bar{\varepsilon}_g|u_{eq}| + |u_0|\right. \\ &\left. - \frac{|s^T|(\bar{s}_f + \bar{s}_g|u_{eq}| + |u_0|)}{\sigma_0\|s\|^2 + \delta}\right).\end{aligned} \quad (39)$$

As a result,

$$s^TG(x)s \geq \sigma_0\|s\|^2 \quad (40)$$

Then, the second term of the Lyapunov candidate function is bounded.

$$\begin{aligned}\dot{V}_2 \leq &-s^TG(x)u_{sliding} \\ &+ |s^T|.\left(\bar{\varepsilon}_f + \bar{\varepsilon}_g|u_{eq}| + |u_0|\right) \\ &+ \frac{1}{\eta_0}\delta\dot{\delta}\end{aligned} \quad (41)$$

$$\dot{V}_2 \leq -\frac{\delta|s^T|(\bar{s}_f + \bar{s}_g|u_{eq}| + |u_0|)}{\sigma_0\|s\|^2 + \delta} + \frac{1}{\eta_0}\delta\dot{\delta} \quad (42)$$

$$\dot{V}_2 \leq 0 \quad (43)$$

From equation (37), we obtain

$$\dot{V} \leq -s^TK_0\, sgn(s) = -(k_1|s_1| + k_2|s_2|) \quad (44)$$

Owing to Barbalat's lemma, it could be concluded that the tracking errors and their derivatives decrease asymptotically to zero, that is $e_i^j(t) \to 0\ as\ t \to \infty\ for\ i,j = 1,2$. Hence, the system stability is proved.

V. Results and Discussions

To verify the performance of the proposed controller, several tests of numerical simulations are carried out. Table 2 indicates the values of parameters to simulate the system performance. The reference input signal is selected as a sinusoidal function $y_{d1} = y_{d2} = sin(t)$. The external disturbances $[cos(t)\ \ sin(t)]^T$ are embedded in this system. The coefficients of the sliding surface are determined as $\lambda_1 = \lambda_2 = 2$. Furthermore, the system parameters for tuning in this simulation are listed $\varepsilon_0 = 0.5, \eta_{f1} = \eta_{f2} = 0.1$, $\eta_{g11} = \eta_{g12} = \eta_{g21} = \eta_{g22} = 0.1$, $K_0 = 0.5I_2$. The design parameters for controllers are well-tuned as $K_P = 10$, $K_I = 0.1$, $K_D = 0.01$ for PID scheme $K_{vff} = 1, K_{aff} = 1$ for Feed-forward scheme and $K_f = 0.7$ for interval type-2 FLS. The saturation unit is selected so that the output voltage to the servo system is in a range of -12V and +12V. The initial state of the robot manipulator is chosen $x(0) = [0\ \ 0\ \ 0\ \ 0]$. In order to evaluate the performance of the proposed scheme, it is essential to compare our controller with the traditional fuzzy control system in the same context.

TABLE II. LIST OF THE SYSTEM PARAMETERS

Parameter	Value
m_1	1
m_e	2
l_1	1
l_{cl}	0.5
l_{ce}	0.6
I_1	0.12
I_e	0.25
δ_e	30°

The control signal of both conventional type-1 FLS and the proposed scheme is demonstrated in Fig. 6 and Fig. 7, respectively. While the first link firmly moves, the second one must suffer unexpected effects, such as unknown load, residual oscillation, or external disturbance. Hence, our attention is inclined to the second link in order to drive the end-effector to the target location. In Fig. 8, the demonstration of the tracking position among these controllers is shown. Although bearing the unwanted factors, both of them make an effort to generate the proper control signal. In the first period of link 1, the conventional type-1 FLS does not perform as well as our scheme. Later, it drives the first link back to the reference trajectory. In the second link, a little bit of oscillation appears that might cause instability for this system since the conventional scheme is effortless to deal with uncertainties. To zoom in on the comparative performance, the tracking error of the two schemes is illustrated in Fig. 9. Although there are not many significant differences to adapt with the unknown fluctuations, which is not well-suited for conventionally

tracking performance, the proposed controller seems to be superior to the traditional method.

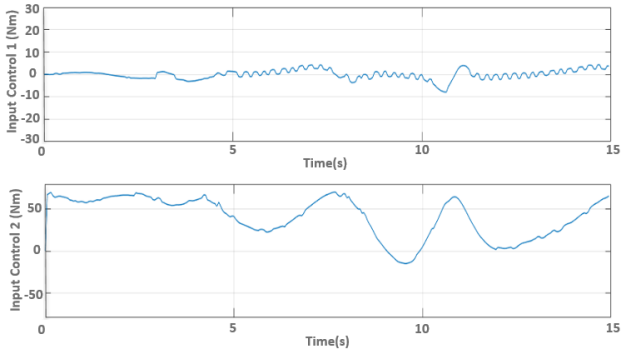

Fig. 6. Validated simulation of a control signal using traditional type-1 FLS for link 1 (above) and link 2 (below) in robot manipulator.

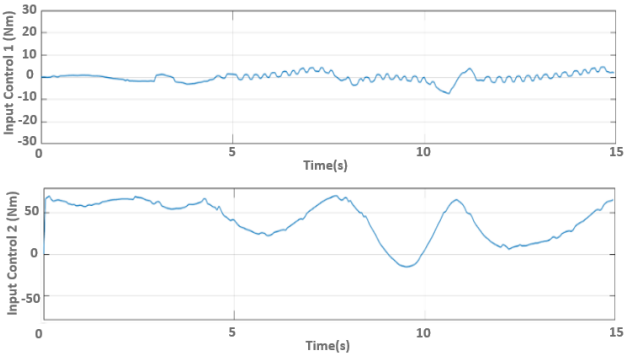

Fig. 7. Validated simulation of a control signal using the proposed controller for link 1 (above) and link 2 (below) in robot manipulator

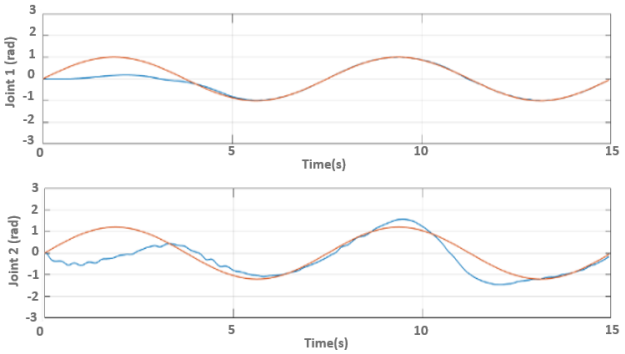

Fig. 8. Comparative simulation of the tracking position between traditional type-1 FLS (blue line) and the proposed controller (red line) for link 1 (above) and link 2 (below) in robot manipulator

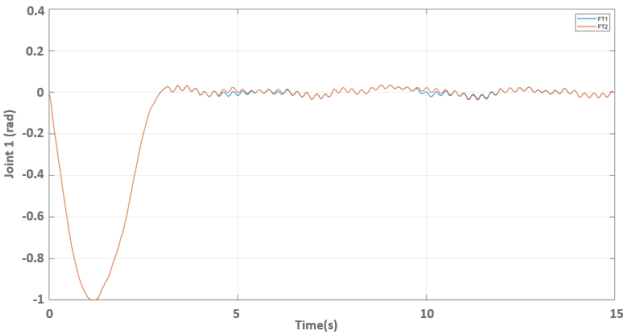

(a)

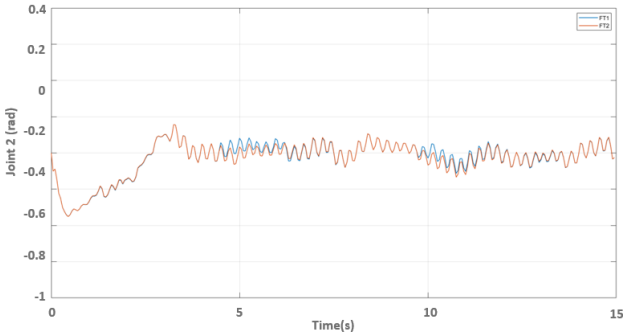

(b)

Fig. 9. Comparative simulation of the tracking error between traditional type-1 FLS (blue line) and the proposed controller (red line) for (b) link 1 and (a) link 2 in robot manipulator

To compare the specifications in different approaches, Table 3 describes the competitive performance and achievements. In such a case, our method is advantageous and provides a robust solution for many industrial applications.

TABLE III. LIST OF COMPARATIVE SPECIFICATIONS BETWEEN OUR METHOD AND THE OTHERS [50, 51]

	Our method	Zhao, T. et al. [50]	Reguli, I. et al. [51]
Application	Manufacturing	Powerline	Navigation
Controller	Type-2 fuzzy sliding mode	Type-2 fuzzy PID	Sliding mode
Advantage(s)	Smaller tracking error	Optimal parameters	Faster time execution
Disadvantage(s)	Burden computation	Burden computation	Static environment

VI. CONCLUSIONS

In this paper, a novel design of both a feed-forward scheme and switching mechanism for robot control was invented. With the advantage of adjusting proactively, the feed-forward control releases an appropriate response at the proper time, and they could minimize the negative effects on the servo system. Additionally, by fusing between the well-known controller such as PID scheme and the advanced controller such as interval type-2 fuzzy sliding mode scheme, the perspective of system response could be improved in real-time characteristic, cutting the burden computation and enhancing the tracking performance while the high level of system specifications such disturbance-rejection is maintained. The intelligent switching mechanism would mostly activate the industrial PID control to drive the servo system when the tracking error is less than the threshold, or it is still far from the target. Otherwise, the interval type-2 fuzzy sliding mode control is deployed to manipulate this system in coping with unknown factors. By using the Lyapunov approach, it is stated that the system stability is guaranteed indefinite time. Several tests are compared with conventional type-1 FLS so that the superior performance of our controller is exhibited. From the points of view of flexible control and robustness, it is clear that our approach is effective and feasible for achieving high-performance control in many applications.

Future work is a must. It requires more investigations on the computational method to reduce the burden theory. Especially in the practical robot system, the motion controller must be generated in real-time. In addition, advanced control schemes such as artificial intelligence or machine learning should be inspected to upgrade.

CONFLICT OF INTEREST

Authors declare that there is no conflict of interest in this study.

ACKNOWLEDGEMENTS

We acknowledge the support of time and facilities from Ho Chi Minh City University of Technology (HCMUT), VNU-HCM for this study.

REFERENCES

[1] K. Mittal, A. Jain, K. S. Vaisla, O. Castillo, and J. Kacprzyk, "A comprehensive review on type 2 fuzzy logic applications: Past, present and future," Engineering Applications of Artificial Intelligence, vol. 95, p. 103916, 2020.

[2] Y. Liu, C. M. Eckert, and C. Earl, "A review of fuzzy AHP methods for decision-making with subjective judgements," Expert Systems with Applications, vol. 161, p. 113738, 2020.

[3] C. Sun, H. Gao, W. He, and Y. Yu, "Fuzzy neural network control of a flexible robotic manipulator using assumed mode method," IEEE Transactions on Neural Networks and Learning Systems, vol. 29, no. 11, 5214-5227, 2018.

[4] H. Han, Y. Wei, X. Ye, and W. Liu, "Modeling and fuzzy decoupling control of an underwater vehicle-manipulator system," IEEE Access, 8, pp. 18962-18983, 2020.

[5] C. Jin, Y. Ren, and G. Zhang, "Interval-valued q-rung orthopair fuzzy FMEA application to improve risk evaluation process of tool changing manipulator," Applied Soft Computing, vol. 104, p. 107192, 2021.

[6] M. A. Sanchez, O. Castillo, and J. R. Castro, "Generalized type-2 fuzzy systems for controlling a mobile robot and a performance comparison with interval type-2 and type-1 fuzzy systems," Expert Systems with Applications, vol. 42, no. 14, pp. 5904-5914, 2015.

[7] S. Dian, Y. Hu, T. Zhao, and J. Han, "Adaptive backstepping control for flexible-joint manipulator using interval type-2 fuzzy neural network approximator," Nonlinear Dynamics, vol. 97, no. 2, pp. 1567-1580, 2019.

[8] P. J. Gaidhane, M. J. Nigam, A. Kumar, and P. M. Pradhan, "Design of interval type-2 fuzzy precompensated PID controller applied to two-DOF robotic manipulator with variable payload," ISA transactions, vol. 89, pp. 169-185, 2019.

[9] H. Qin, H. Yang, Y. Sun, and Y. Zhang, "Adaptive interval type-2 fuzzy fixed-time control for underwater walking robot with error constraints and actuator faults using prescribed performance terminal sliding-mode surfaces," International Journal of Fuzzy Systems, vol. 23, no. 4, pp. 1137-1149, 2021.

[10] X. Zou, T. Zhao, and S. Dian, "Finite-time adaptive interval type-2 fuzzy tracking control for Mecanum-wheel mobile robots," in International Journal of Fuzzy Systems, vol. 24, no. 3, pp. 1570-1585, 2022.

[11] R. Sharma, K. K. Deepak, P. Gaur, and D. Joshi, "An optimal interval type-2 fuzzy logic control based closed-loop drug administration to regulate the mean arterial blood pressure," Computer methods and programs in biomedicine, vol. 185, p. 105167, 2020.

[12] W. Tong, T. Zhao, Q. Duan, H. Zhang, and Y. Mao, "Non-singleton interval type-2 fuzzy PID control for high precision electro-optical tracking system," ISA transactions, vol. 120, pp. 258-270, 2022.

[13] H. Zhou, C. Zhang, S. Tan, Y. Dai, and J. A. Duan, "Design of the footprints of uncertainty for a class of typical interval type-2 fuzzy PI and PD controllers," ISA transactions, vol. 108, pp. 1-9, 2021.

[14] J. E. Moreno, M. A. Sanchez, O. Mendoza, A. Rodríguez-Díaz, O. Castillo, P. Melin, and J. R. Castro, "Design of an interval Type-2 fuzzy model with justifiable uncertainty," in Information Sciences, vol. 513, pp. 206-221, 2020.

[15] M. Van, M. Mavrovouniotis, and S. S. Ge, "An adaptive backstepping nonsingular fast terminal sliding mode control for robust fault tolerant control of robot manipulators," IEEE Transactions on Systems, Man, and Cybernetics: Systems, vol. 49, no. 7, pp. 1448-1458, 2018.

[16] G. M. Méndez, P. N. Montes Dorantes, and M. A. Alcorta, "Dynamic adaptation of the PID's gains via Interval type-1 non-singleton type-2 fuzzy logic systems whose parameters are adapted using the backpropagation learning algorithm," Soft Computing, vol. 24, no. 1, pp. 17-40, 2020.

[17] M. Oussama, C. Abdelghani, and C. Lakhdar, "Efficiency and robustness of type-2 fractional fuzzy PID design using salps swarm algorithm for a wind turbine control under uncertainty," ISA transactions, 2021.

[18] W. C. Su, C. F. Juang, and C. M. Hsu, "Multi-objective Evolutionary Interpretable Type-2 Fuzzy Systems with Structure and Parameter Learning for Hexapod Robot Control," IEEE Transactions on Systems, Man, and Cybernetics: Systems, 2021.

[19] H. Yang, J. Qi, Y. Miao, H. Sun, and J. Li, "A new robot navigation algorithm based on a double-layer ant algorithm and trajectory optimization," IEEE Transactions on Industrial Electronics, vol. 66, no. 11, pp. 8557-8566, 2018.

[20] M. M. Zirkohi, "Adaptive interval type-2 fuzzy recurrent RBFNN control design using ellipsoidal membership functions with application to MEMS gyroscope," ISA transactions, vol. 119, pp. 25-40, 2022.

[21] B. Singh, R. Kumar, and V. P. Singh, "Reinforcement learning in robotic applications: a comprehensive survey," Artificial Intelligence Review, pp. 1-46, 2021.

[22] Y. Liu, and Q. Zhu, "Adaptive fuzzy finite-time control for nonstrict-feedback nonlinear systems," IEEE Transactions on Cybernetics, 2021.

[23] J. Wang, W. Luo, J. Liu, and L. Wu, "Adaptive type-2 FNN-based dynamic sliding mode control of DC–DC boost converters," IEEE transactions on systems, man, and cybernetics: systems, vol. 51, no. 4, pp. 2246-2257, 2019.

[24] A. H. Mazinan, "Interval type-II Takagi–Sugeno fuzzy-based strategy in control of autonomous systems," SN Applied Sciences, vol. 1, no. 11, pp. 1-9, 2019.

[25] M. S. AbouOmar, Y. Su, H. Zhang, B. Shi, and L. Wan, "Observer-based interval type-2 fuzzy PID controller for PEMFC air feeding system using novel hybrid neural network algorithm-differential evolution optimizer," Alexandria Engineering Journal, 2022.

[26] S. Xie, Y. Xie, F. Li, Z. Jiang, and W. Gui, "Hybrid fuzzy control for the goethite process in zinc production plant combining type-1 and type-2 fuzzy logics," Neurocomputing, vol. 366, pp. 170-177, 2019.

[27] M. G. Nampoothiri, B. Vinayakumar, Y. Sunny, and R. Antony, "Recent developments in terrain identification, classification, parameter estimation for the navigation of autonomous robots," SN Applied Sciences, vol. 3, no. 4, pp. 1-14, 2021.

[28] R. Sharma and A. Kumar, "Optimal Interval Type-2 Fuzzy Logic Control Based Closed-Loop Regulation of Mean Arterial Blood Pressure Using the Controlled Drug Administration," IEEE Sensors Journal, vol. 22, no. 7, pp. 7195-7207, 2022.

[29] D. Sain, M. Praharaj, and M. M. Bosukonda, "A simple modelling strategy for integer order and fractional order interval type-2 fuzzy PID controllers with their simulation and real-time implementation," Expert Systems with Applications, vol. 202, p. 117196, 2022.

[30] S. Hou, Y. Chu, and J. Fei, "Adaptive type-2 fuzzy neural network inherited terminal sliding mode control for power quality improvement," IEEE Transactions on Industrial Informatics, vol. 17, no. 11, pp. 7564-7574, 2021.

[31] D. Xuan and J. Bae, "A Precise Neural-Disturbance Learning Controller of Constrained Robotic Manipulators," IEEE Access, vol. 9, pp. 50381-50390, 2021.

[32] J. Liu, T. Zhao, and S. Dian, "General type-2 fuzzy sliding mode control for motion balance adjusting of powerline inspection robot," Soft Computing, vol. 25, no. 2, pp. 1033-1047, 2021.

[33] L. Charron, M. Boumehraz, and A. Kouzou, "Mobile robot path planning based on optimized fuzzy logic controllers," New Developments and Advances in Robot Control, 2019, pp. 255-283.

[34] A. Al-Mahturi, F. Santoso, M. A. Garratt, and S. G. Anavatti, "A robust self-adaptive interval type-2 TS fuzzy logic for controlling multi-input-multi-output nonlinear uncertain dynamical systems," IEEE Transactions on Systems, Man, and Cybernetics: Systems, 2020.

[35] M. B. Milovanović, D. S. Antić, M. T. Milojković, and M. D. Spasić, "Adaptive control of nonlinear MIMO system with orthogonal endocrine intelligent controller," IEEE Transactions on Cybernetics, 2020.

[36] M. H. Chang and Y. C. Wu, "Speed control of electric vehicle by using type-2 fuzzy neural network," International Journal of Machine Learning and Cybernetics, vol. 13, no. 6, pp. 1647-1660, 2022.
[37] C. He, M. Mahfouf, and L. A. Torres-Salomao, "An adaptive general type-2 fuzzy logic approach for psychophysiological state modeling in real-time human–machine interfaces," IEEE Transactions on Human-Machine Systems, vol. 51, no. 1, pp. 1-11, 2020.
[38] G. Enthrakandi Narasimhan, and J. Bettyjane, "Implementation and study of a novel approach to control adaptive cooperative robot using fuzzy rules," International Journal of Information Technology, vol. 13, no. 6, pp. 2287-2294, 2021.
[39] T. L. Le, N. V. Quynh, N. K. Long, and S. K. Hong, "Multilayer interval type-2 fuzzy controller design for quadcopter unmanned aerial vehicles using Jaya algorithm," IEEE Access, vol. 8, pp. 181246-181257, 2020.
[40] P. M. Kebria, A. Khosravi, S. Nahavandi, D. Wu, and F. Bello, "Adaptive type-2 fuzzy neural-network control for teleoperation systems with delay and uncertainties," IEEE Transactions on Fuzzy Systems, vol. 28, no. 10, pp. 2543-2554, 2019.
[41] D. Sun, Q. Liao, T. Stoyanov, A. Kiselev, and A. Loutfi, "Bilateral telerobotic system using type-2 fuzzy neural network based moving horizon estimation force observer for enhancement of environmental force compliance and human perception," Automatica, vol. 106, pp. 358-373, 2019.
[42] Z. Wang, H. K. Lam, B. Xiao, Z. Chen, B. Liang, and T. Zhang, "Event-triggered prescribed-time fuzzy control for space teleoperation systems subject to multiple constraints and uncertainties," IEEE Transactions on Fuzzy Systems, vol. 29, no. 9, pp. 2785-2797, 2020.
[43] Q. Liao, and D. Sun, "Sparse and Decoupling Control Strategies Based on Takagi–Sugeno Fuzzy Models," IEEE transactions on cybernetics, vol. 51 no. 2, pp. 947-960, 2019.
[44] S. Paul, A. Arunachalam, D. Khodadad, H. Andreasson, and O. Rubanenko, "Fuzzy tuned pid controller for envisioned agricultural manipulator," International Journal of Automation and Computing, vol. 18, no. 4, pp. 568-580, 2021.
[45] D. Sun, Q. Liao, and A. Loutfi, "Type-2 Fuzzy Model-Based Movement Primitives for Imitation Learning," IEEE Transactions on Robotics, 2022.
[46] A. Rubio-Solis, U. Martinez-Hernandez, L. Nava-Balanzar, L. G. Garcia-Valdovinos, N. A. Rodriguez-Olivares, J. P. Orozco-Muñiz, and T. Salgado-Jimenez, "Online Interval Type-2 Fuzzy Extreme Learning Machine applied to 3D path following for Remotely Operated Underwater Vehicles," Applied Soft Computing, vol. 115, p. 108054, 2022.
[47] X. Lu, Y. Zhao, and M. Liu, "Self-learning interval type-2 fuzzy neural network controllers for trajectory control of a Delta parallel robot," Neurocomputing, vol. 283, pp. 107-119, 2018.
[48] F. Baghbani, M. R. Akbarzadeh-T, and A. Akbarzadeh, "Indirect adaptive robust mixed H2/H∞ general type-2 fuzzy control of uncertain nonlinear systems," Applied Soft Computing, vol. 72, pp. 392-418, 2018.
[49] J. Z. Shi, "A fractional order general type-2 fuzzy PID controller design algorithm," IEEE Access, vol. 8, pp. 52151-52172, 2020.
[50] T. Zhao, Y. Chen, S. Dian, R. Guo, and S. Li, "General type-2 fuzzy gain scheduling PID controller with application to powerline inspection robots," International Journal of Fuzzy Systems, vol. 22, no. 1, pp. 181-200, 2020.
[51] I. Reguii, I. Hassani, and C. Rekik, "Mobile Robot Navigation Using Planning Algorithm and Sliding Mode Control in a Cluttered Environment," Journal of Robotics and Control (JRC), vol. 3, no. 2, pp. 166-175, 2022.